

Electronic structure, optical and magnetic properties of Co_2FeGe Heusler alloy films

N. V. Uvarov,¹ Y. V. Kudryavtsev,¹ A. F. Kravets,^{2,3, a)} A. Ya. Vovk,⁴ R. P. Borges,⁴ M. Godinho,⁴ and V. Korenivski²

¹⁾*Institute of Metal Physics, National Academy of Sciences of Ukraine, Vernadsky 36, 252680, Kiev-142, Ukraine*

²⁾*Nanostructure Physics, Royal Institute of Technology, 10691 Stockholm, Sweden*

³⁾*Institute of Magnetism, National Academy of Sciences of Ukraine, Vernadsky 36 b, 03142 Kiev, Ukraine*

⁴⁾*CFMC, Department of Physics, University of Lisbon, Campo Grande, Edif. C8, Lisbon, 1749-016 Lisbon, Portugal*

Optical properties of ferromagnetic half-metallic full-Heusler Co_2FeGe alloy are investigated experimentally and theoretically. Co_2FeGe thin films were obtained by DC magnetron sputtering and show the saturation magnetization at $T=10$ K of $m \approx 5.6 \mu_B/\text{f.u.}$, close to the value predicted by the Slater-Pauling rule. First-principles calculations of the electronic structure and the dielectric tensor are performed using the full-potential linearized-augmented-plane-wave method in the generalized gradient (GGA) and GGA+U approximations. The measured interband optical conductivity spectrum for the alloy exhibits a strong absorption band in the 1 - 4 eV energy range with pronounced fine structure, which agrees well with the calculated half-metallic spectrum of the system, suggesting a near perfect spin-polarization in the material.

PACS numbers: 71.20. \pm b, 75.30. \pm m, 78.20. \pm e

I. INTRODUCTION

Heusler alloys (HA) attract significant attention due to their interesting physical properties promising various practical applications in the fields of smart materials and magneto-electronics.¹ Indeed, certain Co_2Fe -based full-Heusler alloys (FHA) are predicted to be ferromagnetic and half-metallic, *i.e.*, exhibiting near 100% spin polarization of the charge carriers at the Fermi level. This property makes Co_2Fe -based FHA's (and Co_2FeGe among them) promising candidates to be used as spin-injectors in spintronic devices. Furthermore, Co_2Fe -based FHA's have the highest Curie temperatures among the known half-metallic ferromagnets. Therefore, fabrication and investigation of the electronic structure and physical properties of Co_2Fe -based FHA films are of fundamental and technological interest.

The Co_2FeGe system and, in particular, films are rather unexplored. Only a few publications discuss the physical properties of non-stoichiometric Co-Fe-Ge alloy films $[(\text{CoFe})_{0.70}\text{Ge}_{0.30}, (\text{CoFe})_{100-x}\text{Ge}_x]$ and spin-valves based on them.²⁻⁴ Full-Heusler $L2_1$ -type ordered $\text{Co}_{45}\text{Fe}_{31}\text{Ge}_{24}$ thin films were successfully fabricated by Takamura, *et al.* using a thermally activated germanidation reaction between ultra-thin germanium-on-insulator and Co-Fe layers deposited on it.⁵ However, such films showed magnetic moments of $m=4.8\mu_B$, which was notably smaller than the bulk value of $m=5.54\mu_B$ ⁶, probably due to their off-stoichiometry.

The important aspect of the half-metallic Heusler alloys is their unique magneto-optical (MO) properties: a

discovery of giant Kerr rotation in half-Heusler PtMnSb alloy opens the way for applications in MO reading-recording.⁷ Optical and MO properties of a number of half-metallic FHA's have been investigated theoretically and experimentally.⁸⁻¹⁷ It has been shown that the predictions significantly depend on the calculation methods employed.^{12,17} At the same time, the experimental optical and MO properties of the HA's are often quite difficult to explain without first-principle calculations. It is preferred, therefore, to combine the two approaches for a comprehensive analysis of a specific material, explaining the measured data at the same time as verifying experimentally the theoretical model used. Optical and magneto-optical properties of Co_2FeGe compound were have been simulated by Kim *et al.* using the generalized gradient approximation (GGA) and GGA+U approaches.¹⁷ It was shown that the predicted properties significantly depend on calculation approach used, so a comparison with the experiment was necessary to validate and, if necessary, refine the alternatives. Therefore, one of the article's purpose is checking the correctness of various calculation tools by the comparison of calculated and experimental physical (optical and magnetic) properties of alloy.

In this work we fabricate the largely unexplored Co_2FeGe alloy in the film form using sputtering, measure their optical and magnetic properties, and develop and refine first-principles models for explaining the data observed. Our results indicate half-metallicity, which should be interesting for a number of applications.

^{a)} Electronic mail: anatolii@kth.se

II. EXPERIMENTAL AND THEORETICAL METHODS

Co_2FeGe Heusler alloy films of 50 nm in thickness were deposited at 500 °C on thermally oxidized Si substrates using DC magnetron co-sputtering from Co_2Fe and Ge targets. The base pressure in the deposition chamber was 5×10^{-8} Torr and the Ar pressure used during deposition was 5 mTorr. The deposition rates for Co_2Fe and Ge components were 0.0781 and 0.0174 nm/sec, respectively. The film composition was determined using x-ray dispersion spectroscopy analysis.

The crystalline structure was analyzed using X-ray diffraction (XRD) in the $\theta-2\theta$ geometry with Cu- K_α radiation of 1.5406 Å wavelength.

Magnetic measurements were performed using a SQUID MPMS-5 magnetometer in the temperature range of 5-300 K. Magnetic field was applied in the film plane. The substrate contribution was subtracted using the methods described by Garcia *et al.*¹⁸

The electronic structure, optical properties such as the dielectric function (DF), and magnetic properties of the Co_2FeGe alloy with $L2_1$ type structure (space group $Fm\bar{3}m$) were calculated using the WIEN2k code¹⁹, utilizing a full-potential linearized-augmented-plane-wave method with GGA and GGA+U methods.²⁰ For the exchange-correlation functional, the generalized-gradient-approximation version of Perdew *et al.*²¹ was used. In the $L2_1$ -type structure Co atoms are located at $(1/4, 1/4, 1/4)$, Fe atoms at $(0.0, 0.0, 0.0)$ and Ge atoms at $(1/2, 1/2, 1/2)$ in the unit cell of a 225 space group.

The cell size was determined in the calculations from minimizing the full electron energy versus the lattice parameter. Self-consistency was obtained using 816 k-points in the irreducible Brillouin zone (IBZ). To calculate the DF of Co_2FeGe we used 4285 k-points in the IBZ.

The calculated optical properties of the Co_2FeGe HA were compared with the experimental ones. Optical properties, such as $[Re(\sigma) = \omega\epsilon_2/4\pi]$ and ϵ_1 , where σ is the optical conductivity (OC), ϵ_1 and ϵ_2 the real and imaginary parts of the diagonal components of the DF $\tilde{\epsilon} = \epsilon_1 - i\epsilon_2$ of the samples were measured using a spectroscopic rotating analyzer-ellipsometer, at 293 K, in the spectral range of 310 - 2500 nm (4.0 - 0.5 eV) at a fixed incidence angle of 73°.

III. RESULTS AND DISCUSSION

The calculated density of the electronic states (DOS) for Co_2FeGe alloy with the $L2_1$ -type crystal structure and the lattice parameter of $a=5.75$ Å, obtained using the GGA and GGA + U approaches, are shown in Fig. 1. It is seen that the main contributions to the resulting DOS of Co_2FeGe alloy obtained by either GGA or GGA+U methods are due to the Co and Fe atoms. The Co and Fe states are hybridized - the most intense peaks of the DOS are formed by the coincident in energy Co and Fe

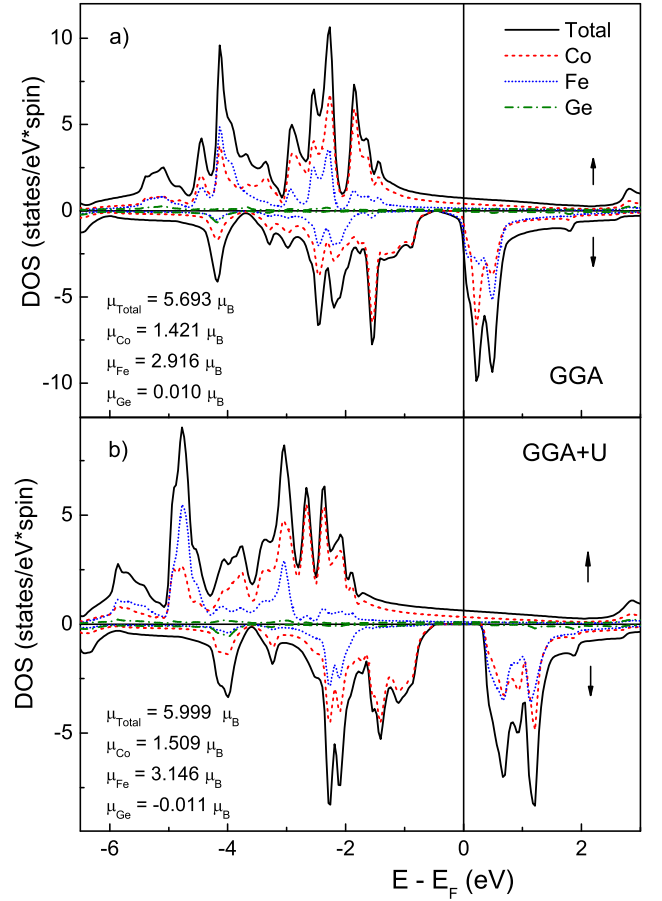


FIG. 1. Spin-resolved DOS for $L2_1$ -phase of Co_2FeGe FHA, calculated using a) GGA and b) GGA+U approximations.

states. A detailed analysis shows that the contribution to the hybridized states is due mainly to the Co and Fe 3d states, which indicates a covalent character of their interaction. The contribution to the total DOS from the Ge states is small. This means that the Ge atoms form essentially ionic bonds with the surrounding atoms.

For the minority bands both approaches reveal a deep minimum (GGA) or even an energy gap of about 1 eV at the Fermi level (GGA+U). Thus, GGA+U predicts Co_2FeGe HA to be a half-metal with the spin polarization of $P=1.000$, while GGA predicts still a rather high $P=0.504$.

The DOS shown in Fig. 1 agree well with the results in the literature obtained for $L2_1$ -type ordered Co_2MnGe using LDA, LDA+U, GGA, and GGA+U.^{12,17,22,23}

The GGA and GGA+U methods reveal somewhat different values of the magnetic moment of the alloy. According to the Slater-Pauling rule,^{24,25} $L2_1$ -type Co_2FeGe HA should have a magnetic moment of $\mu_{\text{Co}_2\text{FeGe}} = N - 24 = 6\mu_B$, where $N = 2\text{Co}(3d^7 4s^2) + \text{Fe}(3d^6 4s^2) + \text{Ge}(4s^2 4p^2) = 30$. The GGA+U result for the magnetic moment is almost exactly that expected from Slater-Pauling, $m_{\text{Co}_2\text{FeGe}} = 5.999\mu_B$, $\text{Co}=1.509\mu_B$, $\text{Fe}=3.146\mu_B$, $\text{Ge}=-0.011\mu_B$, while GGA

yields $m_{LDA} = 5.693 \mu_B$ (see Fig. 1 b).

Approximately the same difference between the magnetic moments of Co_2FeGe calculated using LDA (GGA) and LDA+U (GGA+U) can be found in the literature. Thus, Kandpal *et al.* report the total magnetic moment of the alloy of $m_{\text{Co}_2\text{FeGe}} = 5.72 \mu_B/\text{f.u.}$ (Co= $1.42 \mu_B$, Fe= $2.92 \mu_B$).²⁶ Kumar *et al.* calculate for Co_2FeGe the total magnetic moment of $m_{\text{Co}_2\text{FeGe}} = 5.72 \mu_B/\text{f.u.}$ (Co= $1.43 \mu_B$, Fe= $2.88 \mu_B$, Ge= $0.01 \mu_B$) and $6.02 \mu_B/\text{f.u.}$ (Co= $1.53 \mu_B$, Fe= $3.12 \mu_B$, Ge= $-0.03 \mu_B$), for GGA and GGA+U, respectively.^{12,22} These values for the magnetic moments in Co_2FeGe , obtained using both LDA and GGA, are in good agreement with the experimental values: $m_{\text{exp}} = 5.54, 5.70$ or $5.74 \mu_B/\text{f.u.}$ ^{6,22,27}

Taking into account that the magnetic moment of Co_2FeGe obtained using the GGA+U approach fits better the Slater-Pauling rule than does the moment in the GGA approximation, we calculate the optical properties of Co_2FeGe using GGA+U.

Because of rather small Co_2FeGe alloy films thickness (50 nm) their composition was examined by employing both energy-dispersive X-ray spectrometer of JEOL JSM-6490LV and wavelength dispersive X-ray spectrometer of JEOL JXA-8200. Aforementioned tools revealed a composition (in atomic percent) of $\text{Co}_{55.7}\text{Fe}_{24.0}\text{Ge}_{20.3}$ and $\text{Co}_{59.7}\text{Fe}_{26.5}\text{Ge}_{13.8}$ (hereafter Co_2FeGe), respectively.

The X-ray diffraction pattern for a Co_2FeGe film deposited on a thermally oxidized Si substrate is shown in Fig. 2. Additional to the reflection peaks of the Si substrate, only one diffraction peak of Co_2FeGe is present. It corresponds to a (220) diffraction peak of a cubic structure and connected with a non-epitaxial growth of the Co_2FeGe film.⁵ The deposited film grows on the amorphous SiO_2 surface that does not provide favourable conditions for epitaxy. The lattice parameter derived using Bragg's law is $a = 5.702 \text{ \AA}$. This value is slightly lower than those determined experimentally for bulk stoichiometric Co_2FeGe alloy ($a = 5.738 \text{ \AA}$ or $a = 5.743 \text{ \AA}$).^{6,28} Applying the volume correction to our data yields $a = 5.75 \text{ \AA}$.

Magnetic hysteresis loops for a Co_2FeGe film measured at different temperatures are shown in Fig. 3. The film demonstrates ferromagnetic properties in the whole investigated temperature range. The saturation magnetization practically does not change with temperature from 10 to 300 K, decreasing only by $\sim 3\%$ (from 1120 emu/cc to 1090 emu/cc). Such behavior of magnetization-vs-temperature indicates a high Curie temperature T_C of the alloy. Taking into account that Co_2FeGe FHA have four atoms per unit cell and applying the experimental values of the saturation magnetization (M_s) at $T = 10 \text{ K}$ and the lattice parameter one obtains $M_s \approx 5.6 \mu_B/\text{f.u.}$ This value is very close to that predicted by the Slater-Pauling rule (*i.e.* $6.0 \mu_B/\text{f.u.}$) as well as that calculated using the GGA+U approach. It should also be pointed out that Co_2FeGe films have relatively low coercivity, which increases from $H_c \sim 15 \text{ Oe}$ to 45 Oe when the temperature decreases from 300 down to 10 K. This fact implies fine-grain crystalline structure of the samples.

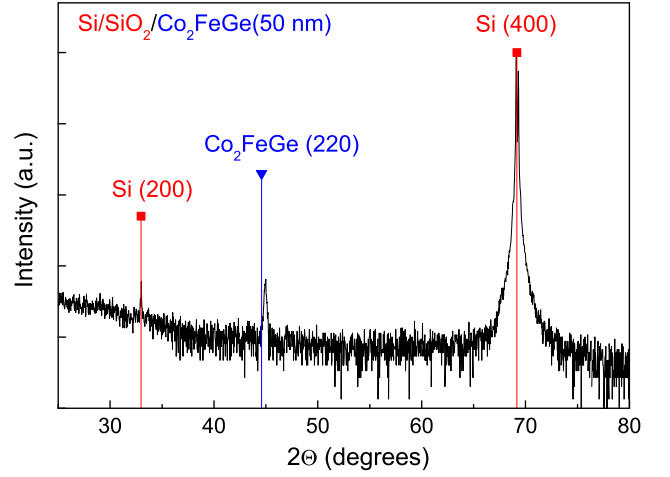


FIG. 2. XRD pattern of a Co_2FeGe film deposited on a thermally oxidized Si substrate.

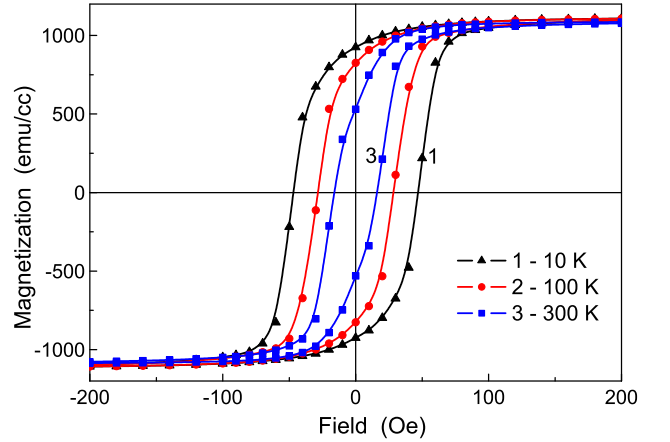


FIG. 3. Magnetic hysteresis loops of a Co_2FeGe film measured at different temperatures with the magnetic field applied in the film plane.

On the basis of the rather good agreement between the experimental and the calculated magnetic moments of Co_2FeGe alloy one can expect that this alloy should exhibit a high degree of spin polarization, predicted by the GGA+U results.

Figures 4 and 5 show the measured and calculated optical properties of the Co_2FeGe alloy. The experimental optical conductivity spectrum exhibits a strong absorption peak in the $0.5 < \hbar\omega < 3.5 \text{ eV}$ energy range, with superposed smaller peaks marked by A - F (see Fig. 4). The theoretical optical properties were obtained using the GGA+U approach. A visual comparison of the experimental $\sigma(\hbar\omega)$ spectrum with calculated one allows us to conclude that they are in good qualitative agreement. A slight shift in energy is the common occurrence originating from some uncertainty of determining the ground level energy in the GGA+U calculation. A good qualitative agreement between the experimental and calculated spectra is found also for the real part of the diagonal

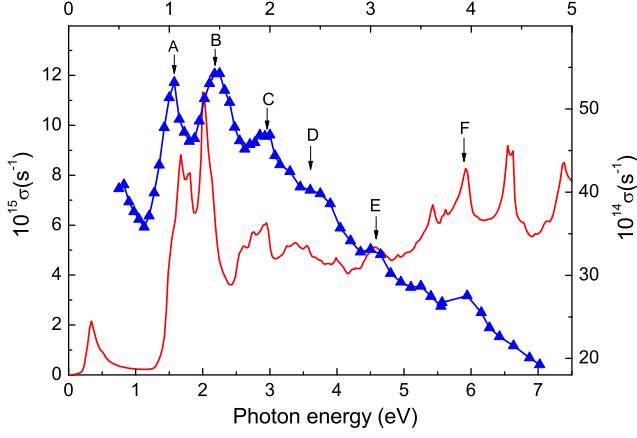


FIG. 4. Experimental (triangles, right and top scales) and calculated (line, left and bottom scales) optical conductivity spectra of Co_2FeGe alloy film.

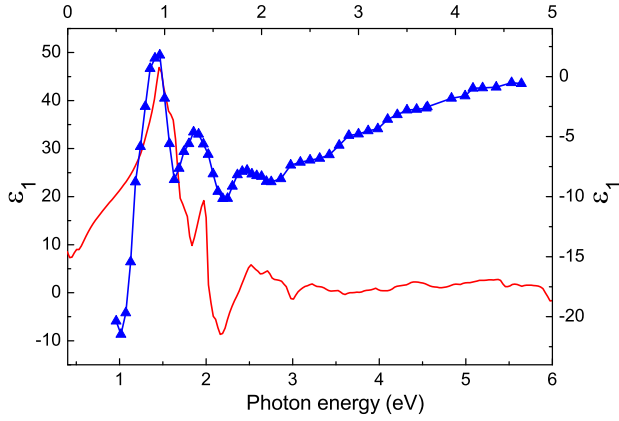


FIG. 5. Experimental (triangles, right and top scales) and calculated (line, left and bottom scales) ϵ_1 spectra of Co_2FeGe alloy film.

components of the DF, $\epsilon_1(\hbar\omega)$, shown in Fig. 5. The intraband contributions to the calculated $\sigma(\hbar\omega)$ and $\epsilon_1(\hbar\omega)$ were not included, which can be the cause of some differences in the peak positions between the calculated and experimental $\sigma(\hbar\omega)$ spectra.

Figures 6 and 7 show the calculated interband optical conductivity spectra with partial contributions from the electron excitations from the various occupied minority and majority bands to unoccupied ones. The main contributions to the most intense experimental interband absorption peaks A and B in Fig. 4 are due to the electron transitions from the 24th, 25th and 26th minority bands (Fig. 6) to all unoccupied bands. These transitions take place between nearly parallel bands in the vicinity of high symmetry points L and Γ , shown in Fig. 8. Peak C at $\hbar\omega=2$ eV in the experimental optical conductivity spectrum (Fig. 4) results mainly from the electron excitations from the majority 33rd band (Fig. 7) to all unoccupied bands in the vicinity of the high-symmetry point K (Fig.

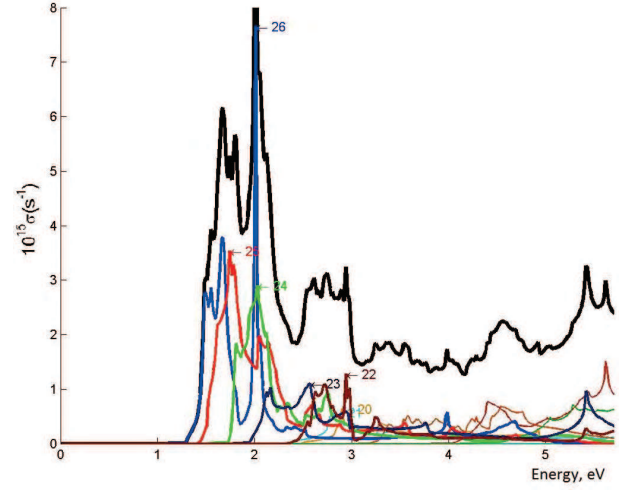


FIG. 6. Calculated total (thick black solid line) and partial contributions to the interband optical conductivity spectrum, produced by electron excitations within the spin-down (minority) sub-bands of the Co_2FeGe FHA.

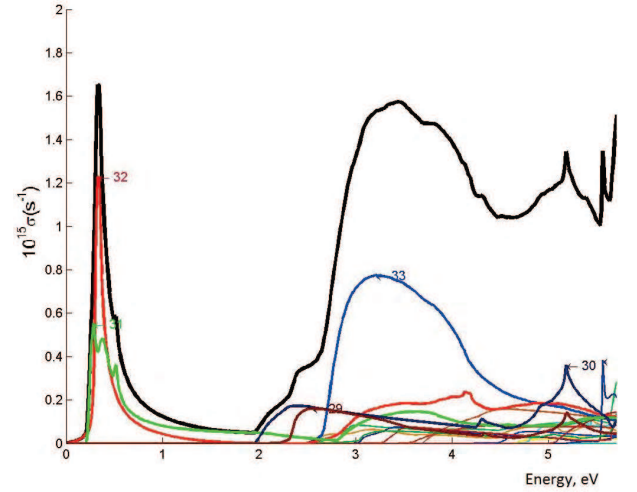


FIG. 7. Calculated total (thick black solid line) and partial contributions to the interband optical conductivity spectrum, produced by electron excitations within the spin-up (majority) sub-bands of the Co_2FeGe FHA.

9). The interband transitions in the minority bands have sharp edges at $\hbar\omega=1.2$ eV.

Unlike electron transitions within minority bands, there is rather intense and very narrow absorption peak at $\hbar\omega=0.5$ eV (see Fig. 7) due to the electron excitations from the 31st and 32nd bands within majority bands (Fig. 9). This peak is not observed experimentally because it is outside of the measuring range. Absorption peaks D - F in the experimental $\sigma(\hbar\omega)$ spectrum (Fig. 4) are due to electronic transitions in both the minority and majority bands, as can be seen in Figs. 6 and 7).

The experimental $\epsilon_1(\hbar\omega)$ spectrum shows generally the Drude-like behavior, *i.e.*, increase in the absolute value

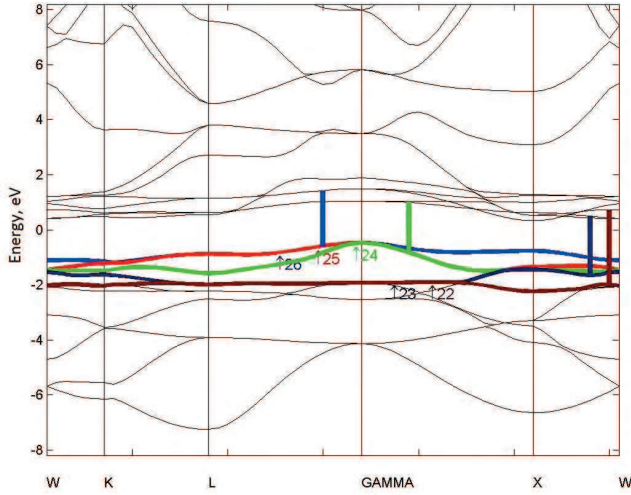


FIG. 8. Spin-down (minority) band structure of Co_2FeGe FHA. The most intense electron transitions are marked by arrows.

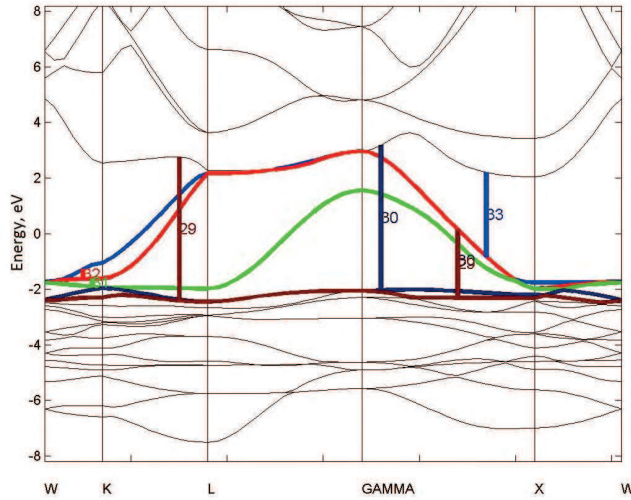


FIG. 9. Spin-up (majority) band structure of Co_2FeGe FHA. The most intense electron transitions are marked by arrows.

being negative with decreasing photon energy. This general dependence is modulated by the anomalous dispersion regions near the most intense absorption peaks due to electronic transitions in the system (Fig. 5).

IV. CONCLUSIONS

Nearly stoichiometric Co_2FeGe Heusler alloy films have been fabricated using DC-magnetron co-deposition from Co_2Fe and Ge targets. The saturation magnetization of the material is measured to be close to that predicted by the Slater-Pauling rule. The measured optical properties are well explained in terms of the alloy's band structure, calculated ab-initio using the GGA+U approach, and

found to correspond to a half-metallic ferromagnet. The half-metallicity of the obtained material may prove useful for applications in spin-polarizers and spin-injectors in magnetic nanodevices.

ACKNOWLEDGMENTS

We gratefully acknowledges support from project EU-FP7-FETOpen-STELE, support by the Ukrainian National program "Fundamental problems of nanostructural systems, nanomaterials and nanotechnologies" project 28/12-H. Work of A.Ya. Vovk and P.R. Borges was supported by Portuguese FCT through "Ciencia 2008" and "Ciencia 2007" programs, respectively.

- ¹T. Graf, C. Felser, and S. S. P. Parkin, *Progress in Solid State Chemistry*, **39**, 1 (2011).
- ²S. Maat, M. J. Carey, and J. R. Childress, *Appl. Phys. Lett.* **93**, 143505 (2008).
- ³M. Zhu, B. D. Soe, R. D. McMichael, M. J. Carey, S. Maat, and J. R. Childress, *Appl. Phys. Lett.* **98**, 072510 (2011).
- ⁴H. Lee, Y.-H. Wang, C. K. A. Mewes, W. H. Butler, T. Mewes, S. Maat, B. York, M. J. Carey, and J. R. Childress, *Appl. Phys. Lett.* **95**, 082502 (2009).
- ⁵Y. Takamura, A. Nishijima, Y. Nagahama, R. Nakane, and S. Sugahara, *ECS Transactions*, **16**, 945 (2008).
- ⁶K. H. J. Buschow, P. G. van Engen, and R. Jongebreur, *J. Magn. Magn. Mater.* **38**, 1 (1983).
- ⁷P. G. Van Engen, K. H. J. Buschow, R. Jongebreur, and M. Erman, *Appl. Phys. Lett.* **42**, 202 (1983).
- ⁸Y. Kubo, N. Takakura, and S. Ishida, *J. Phys. F: Met. Phys.* **13**, 161 (1983).
- ⁹S. Picozzi, A. Continenza, and A. J. Freeman, *Jour. Phys. D: Appl. Phys.* **39**, 851 (2006).
- ¹⁰F. Ricci, S. Picozzi, A. Continenza, F. D'orazio, F. Lucari, K. Westerhold, M. Kim, and A. J. Freeman, arXiv07063613v1 [cond-mat.mtrl-sci] 25 Jun 2007.
- ¹¹K. A. Fomina, V. V. Marchenkov, E. I. Shreder, and H. W. Weber, *Solid State Phenomena*, **168-169**, 545 (2011).
- ¹²M. Kumar, T. Nautiyal, and S. Auluck, *J. Phys.: Condens. Matter* **21**, 196003 (2009).
- ¹³E. Shreder, S. V. Streltsov, A. Svyazhyn, A. Makhnev, V. V. Marchenkov, A. Lukoyanov, and H. W. Weber, *J. Phys. Condens. Matter* **20**, 045212 (2008).
- ¹⁴E. I. Shreder, A. D. Svyazhyn, and K. A. Fomina, *Physics of Metals and Metallography*, **113**, 155 (2012).
- ¹⁵S. Naderizadeh, S. M. Elahi, M. R. Abolhassani, F. Kanjouri, N. Rahimi, and J. Jalilian, *Eur. Phys. J. B* **85**, 144 (2012).
- ¹⁶B. Xu and L. Liu, *J. Phys. D: Appl. Phys.* **41**, 095404 (2008).
- ¹⁷M. Kim, H. Lim, and J. I. Lee, *Thin Solid Films*, **519**, 8419 (2011).
- ¹⁸M. A. Garcia, E. Fernandez Pinel, J. de la Venta, A. Quesada, V. Bouzas, J. F. Fernandez, J. J. Romero, M. S. Martin Gonzalez, and J. L. Costa-Kramer, *J. Appl. Phys.* **105**, 013925 (2009).
- ¹⁹P. Blaha, K. Schwarz, G. K. H. Madsen, D. Kvasnicka, and J. Luitz, *WIEN2k, An Augmented Plane Wave + Local Orbitals Program for Calculating Crystal Properties* (Karl-heinz Schwarz, Techn. Universit Aat Wien, Wien, Austria, 2001).
- ²⁰E. Wimmer, H. Krakauer, M. Weinert, and A. J. Freeman, *Phys. Rev. B* **24**, 864 (1981).
- ²¹J. P. Perdew, K. Burke, and M. Ernzerhof, *Phys. Rev. Lett.* **77**, 3865 (1996).
- ²²K. R. Kumar, K. K. Bharathi, J. A. Chelvane, S. Venkatesh, G. Markandeyulu, and N. Harishkumar, *IEEE Transactions on Magnetics*, **45**, 3997 (2009).
- ²³B. Balke, S. Wurmehl, G. H. Fecher, C. Felser, and J. Kübler, *Sci. Technol. Adv. Mater.* **9**, 014102 (2008).
- ²⁴J. C. Slater, *Phys. Rev.* **36**, 931 (1936).
- ²⁵L. Pauling, *Phys. Rev.* **54**, 899 (1938).
- ²⁶H. C. Kandpal, G. H. Fecher, and C. Felser, *J. Phys. D: Appl. Phys.* **40**, 1507 (2007).
- ²⁷M. Sargolzaei, M. Richter, K. Koepernik, I. Opahle, H. Eschrig, and I. Chaplygin, *Phys. Rev. B* **74**, 224410 (2006).
- ²⁸B. Balke, S. Wurmehl, G. H. Fecher, C. Felser, M. C. Alves et al., *Appl. Phys. Lett.* **90**, 172501 (2007).
- ²⁹B. Balke, G. H. Fecher, and C. Felser, *LNLS 2006 Activity Report*.